PHYSICAL REVIEW E **80**, 065302(R) (2009)

Water wave collapses over quasi-one-dimensional nonuniformly periodic bed profiles

V. P. Ruban*
Landau Institute for Theoretical Physics, 2 Kosygin Street, 119334 Moscow, Russia
(Received 19 October 2009; published 30 December 2009)

Nonlinear water waves interacting with quasi-one-dimensional nonuniformly periodic bed profiles are studied numerically in the deep-water regime with the help of approximate equations for envelopes of the forward and backward waves. Spontaneous formation of localized two-dimensional wave structures is observed in the numerical experiments, which looks essentially as a wave collapse.

DOI: 10.1103/PhysRevE.80.065302 PACS number(s): 47.15.K−, 47.35.Bb, 47.35.Lf

Nonlinear waves of different nature, when propagating in spatially periodic media, are known to introduce various interesting phenomena. In particular, the so-called gap solitons (GSs) can be mentioned, which are self-localized waves existing due to the presence of a Bragg gap in the spectrum of linear waves, and, on the other hand, due to nonlinear interactions between components of the wave field. Gap solitons are studied mainly in the nonlinear optics (see, e.g., Refs. [1–11]), and in the theory of Bose-Einstein condensation [12–14]. However, recently it has been suggested that water wave GSs are possible too, over periodic bottom boundary [15,16]. In the cited works [15,16], planar potential flows with one-dimensional (1D) free boundary were studied both analytically—with the help of an approximate model possessing relatively simple particular solutions, and numerically—exact equations of motion for an ideal fluid with a free surface over a nonuniform bed were simulated, in terms of the so-called conformal variables (see Ref. [17]). For two horizontal dimensions, the question about possibility of GSs or some other coherent water wave structures over periodic bed profiles is still open. The present work is a step to study this problem. More specifically, we suggest here approximate equations of motion for a two-dimensional (2D) free surface over a quasi-one-dimensional, locally periodic nonuniform bed. Then we present some numerical results where spontaneous formation of localized nonlinear structures is clearly seen, and the process looks as a kind of wave collapse. It should be emphasized that the Bragg interaction between the forward wave and the backward wave plays the key role in this process, since the wave dynamics over a flat bottom is rather different, and the extreme waves there are not as high as they are with the Bragg interaction. It is quite possible that effects considered in the present work have in some cases relation to the extensively discussed phenomenon of rogue waves [18,19], namely, at seas with a nonuniform depth of ~50–100 m.

Analytical and numerical results of Ref. [16] imply that the most suitable asymptotic regime for observation of nonlinear Bragg structures of the GS type in water wave systems is the relatively short-wave (or deep-water) regime, when an effective water depth h_0 and the main Bragg-resonant wave number κ form a small parameter $\varepsilon \equiv \exp(-2\kappa h_0) \sim 0.01$. It should be noted here that the opposite long-wave asymptotic regime is very different and typical nonlinear structures at shallow water are KdV-type solitons (see Refs. [20,21]). In the considered deep-water regime, one can use the fourth-order Hamiltonian functional $\mathcal{H}\{\eta,\psi\}$ for weakly nonlinear gravity water waves in the approximate form (see Ref. [16]),

$$\mathcal{H} \approx \frac{1}{2}\int \{\psi\hat{K}\psi + g\eta^2 + \eta[(\nabla\psi)^2 - (\hat{k}\psi)^2]\}d^2\mathbf{r} + \frac{1}{2}\int [\psi\hat{k}\eta\hat{k}\eta\hat{k}\psi + \eta^2(\hat{k}\psi)\nabla^2\psi]d^2\mathbf{r}, \tag{1}$$

where $\mathbf{r}=(x,y)$ is the position in the horizontal plane, g is the gravity acceleration, the canonical variables $\eta(\mathbf{r},t)$ and $\psi(\mathbf{r},t)$ are the vertical coordinate of the free surface and the boundary value of the velocity potential, respectively, the linear operator $\hat{k}=(\hat{k}_x^2+\hat{k}_y^2)^{1/2}$ is diagonal in the Fourier representation, and $\hat{K}=\hat{k}+\hat{B}$ is a linear operator connecting the velocity potential $\varphi(x,y,z=0)$ at the unperturbed free surface and the quantity $\partial_z\varphi(x,y,z=0)$, in the presence of an inhomogeneous bed. The operator $\hat{B}$ depends on a given bed profile in a complicated manner (see Refs. [16,22], where some expansions of this operator are discussed), but it is definitely "small" in the deep-water limit, $\hat{B}\sim\varepsilon$, and that is why we keep $\hat{B}$ only in the quadratic part of the Hamiltonian, while in all higher-order terms we write $\hat{k}$ instead of $\hat{K}$.

Canonical equations of motion, corresponding to Hamiltonian (1), are still too complicated to be treated analytically and very time-demanding when being solved numerically. Therefore we shall consider here a simplified model which can be derived from Eq. (1) in some limit. To do this, let us recall the well-known fact that a suitable weakly nonlinear canonical transformation,

$$b_{\mathbf{k}} = \frac{\sqrt{g}\,\eta_{\mathbf{k}} + i\sqrt{|\mathbf{k}|}\,\psi_{\mathbf{k}}}{\sqrt{2\omega_{\mathbf{k}}}} + \text{nonlinear terms}, \tag{2}$$

(where $\omega_{\mathbf{k}}=(g|\mathbf{k}|)^{1/2}$ is a linear dispersion relation in the absence of the bottom boundary) can exclude the third-order terms from the infinitely deep-water Hamiltonian, as well as the nonresonant wave interactions $0\leftrightarrow 4$ and $1\leftrightarrow 3$ (see Refs. [23,24]). Accordingly, the shape of the free surface $\eta(x,y,t)$ is given by the formula below:

$$\eta(\mathbf{r},t) = \mathrm{Re}\int (2\omega_{\mathbf{k}}/g)^{1/2} b_{\mathbf{k}}(t) e^{i\mathbf{k}\mathbf{r}} d\mathbf{k}/(2\pi) + \cdots. \tag{3}$$

*ruban@itp.ac.ru

When $\hat{B} \neq 0$, some third- and higher-order terms remain in the transformed Hamiltonian, but they are negligible as being proportional to ε. Not important in the main approximation are also terms such as bb and b^*b^*. Thus, the weakly nonlinear wave dynamics in deep-water regime is described by the following integral equation,

$$i\dot{b}_{\mathbf{k}} \approx \omega_{\mathbf{k}} b_{\mathbf{k}} + \hat{L} b_{\mathbf{k}} + \cdots + \frac{1}{2}\int T(\mathbf{k},\mathbf{k}_2;\mathbf{k}_3,\mathbf{k}_4) b^*_{\mathbf{k}_2} b_{\mathbf{k}_3} b_{\mathbf{k}_4} \times \delta(\mathbf{k}+\mathbf{k}_2-\mathbf{k}_3-\mathbf{k}_4) d\mathbf{k}_2 d\mathbf{k}_3 d\mathbf{k}_4, \quad (4)$$

where $\hat{L}$ is a small" linear nondiagonal operator related to $\hat{B}$ and $T(\mathbf{k}_1,\mathbf{k}_2;\mathbf{k}_3,\mathbf{k}_4)$ is a known continuous function (but the corresponding explicit expression is rather complicated, see Refs. [23,24]). For our purposes it is sufficient to know that in purely one-dimensional case

$$T(k_1,k_2;k_1,k_2) \propto |k_1|\,|k_2|(|k_1+k_2|-|k_1-k_2|), \quad (5)$$

and thus $T(k,-k;k,-k)=-T(k,k;k,k)<0$.

Let us assume for the moment that a bed profile is strictly x periodic, with the period $\Lambda=\pi/\kappa$ and one-dimensional (1D) wave spectrum is concentrated near the Bragg-resonant wave vectors $\pm\mathbf{k}_0=\pm\kappa\mathbf{e}_x$. We present two slowly x-dependent functions, the envelopes $A_\pm(x,t)$ of the forward- and backward-propagating waves,

$$\eta(x,t) = \mathrm{Re}[A_+ \exp(i\kappa x - i\tilde{\omega}t) + A_- \exp(-i\kappa x - i\tilde{\omega}t)],$$

where $\tilde{\omega}=(g\kappa)^{1/2}$ (the corresponding deep-water wave period is $T_0=2\pi/\tilde{\omega}$). Then we take into account only the main-order components of the integral operator $\hat{L}$: $L_{\mathbf{k}_0,\mathbf{k}_0}=L_{-\mathbf{k}_0,-\mathbf{k}_0}=-\tilde{\omega}\varepsilon$ and $L_{\mathbf{k}_0,-\mathbf{k}_0}=L^*_{-\mathbf{k}_0,\mathbf{k}_0}=\tilde{\omega}\Delta$, where ε is a real positive number, which should be identified as $\varepsilon=\exp(-2\kappa h_0)$ {it is the definition of h_0 since the finite-depth dispersion relation is $\omega=[g\kappa\tanh(h_0\kappa)]^{1/2}\approx\tilde{\omega}[1-\exp(-2\kappa h_0)]$}; a complex parameter $\Delta=|\Delta|\exp(i\phi)$ bears information about the width of the main Bragg gap, namely, the edges of the frequency gap are at $\omega_{1,2}\approx\tilde{\omega}(1-\varepsilon\mp|\Delta|)$ and about the phase ϕ of the main Fourier harmonics of the bed undulation in some suitable representation (see Ref. [16] for details). It is worth mentioning that for all 1D bed profiles considered in the previous studies [15,16], the inequality $|\Delta|<\varepsilon$ holds ($|\Delta|$ approaches ε from the below if the bottom boundary consists of very narrow barriers).

As a result of the standard procedure, we obtain the system of two coupled approximate equations for the wave envelopes $A_\pm(x,t)$ (compare to Ref. [16]),

$$i\left(\frac{\partial_t}{\tilde{\omega}} \pm \frac{\partial_x}{2\kappa} - \frac{\partial_x^2}{8\kappa^2} + \cdots\right)A_\pm = |\Delta|e^{\pm i\phi}A_\mp - \varepsilon A_\pm + \frac{\kappa^2}{2}(|A_\pm|^2 - 2|A_\mp|^2)A_\pm, \quad (6)$$

where the dots mean higher-order x derivatives. For very narrow spectra, when $|k_x|/\kappa \lesssim |\Delta|^{2/3}$, the dominating dispersion is due to the Bragg coupling and the ∂_x^2 terms are not principal [16]. The above equations describe weakly nonlinear 1D water wave GSs quite well. Known solitary-wave solutions of this system (without the ∂_x^2 terms) were compared in Ref. [16] to numerical simulations of the exact equations of motion for an ideal fluid with a free surface, and a reasonable correspondence was found.

Now it is clear how to generalize the above system to a weakly 2D case: in the usual way we have to add ∂_y-dependent terms to the left hand sides, which appear from expansions of the "shifted" exact dispersive operators $\{-\kappa^{-1/2}[(-i\partial_x\pm\kappa)^2-\partial_y^2]^{1/4}+1\}$. Moreover, we shall consider here the case when ε and Δ are no longer constants, but they are some functions slowly depending on the horizontal coordinates x and y. Technically, this is possible because the kernel $B(\mathbf{r}_1,\mathbf{r}_2)$ of operator $\hat{B}$ rapidly decays if $|\mathbf{r}_1-\mathbf{r}_2|\gtrsim h_0$. The weak nonuniformity of ε and Δ makes our model more realistic and rich, since there is no perfectly periodic bed structures in the nature, while roughly periodic bars are quite often. Then the following natural generalization of Eq. (6) is derived,

$$\left(\frac{i\partial_t}{\tilde{\omega}} \pm \frac{i\partial_x}{2\kappa} - \frac{\partial_x^2}{8\kappa^2} + \frac{\partial_y^2}{4\kappa^2} + \cdots\right)A_\pm = -\varepsilon(x,y)A_\pm + |\Delta(x,y)|e^{\pm i\phi(x,y)}A_\mp + \frac{\kappa^2}{2}(|A_\pm|^2 - 2|A_\mp|^2)A_\pm, \quad (7)$$

where the dots mean omitted third- and higher-order partial derivatives. We keep here the second-order x derivatives because they are definitely important in the dynamics of relatively short-wave groups, when $|\Delta|^{2/3}\lesssim|k_x|/\kappa\ll 1$. The linear and nonlinear terms in the right-hand sides of Eq. (7) are of the same order of magnitude at $\kappa|A_\pm|\sim 0.1$ and $\varepsilon\sim|\Delta|\sim 0.01$ (let us note that water waves become strongly nonlinear if $\kappa|A_\pm|\gtrsim 0.3$).

It should be emphasized that a (spatially nonuniform) linear Bragg coupling between the forward wave and the backward wave introduces essentially effects in the dynamics, in comparison with the flat-bottom case. It is already seen from the linear-wave dispersion relations corresponding to the simplest case $\varepsilon=\mathrm{const}$ and $\Delta=\mathrm{const}>0$. There are two branches in the spectrum (type-1 and type-2 waves), behaving quite nontrivially,

$$\tilde{\omega}^{-1}\Omega_{1,2}(\mathbf{k}) = -\varepsilon \pm \sqrt{\Delta^2 + \frac{k_x^2}{4\kappa^2}} + \frac{k_y^2}{4\kappa^2} - \frac{k_x^2}{8\kappa^2} + \cdots. \quad (8)$$

It is worth noting that the second derivative $\partial^2\Omega_1(k_x,0)/\partial k_x^2$ is positive at small $|k_x|$, while it is negative at $|k_x|/\kappa\gtrsim 2|\Delta|^{2/3}$. Thus the Bragg coupling dominates in the region $|k_x|/\kappa \lesssim |\Delta|^{2/3}$ and $|k_y|/\kappa\lesssim|\Delta|^{1/2}$. It is important that action of the nonlinearity is focusing in both x and y directions at very long spatial scales, if $A_+\approx A_-$. This situation corresponds to a long-scale modulational instability of type-1 waves, which completely surrounds the wave vector $\mathbf{k}=0$, unlike the situation for oppositely propagating waves at infinitely deep water (see, e.g., Refs. [25,26]). Therefore the tendency toward spontaneous formation of big localized waves is stronger if the bottom is (locally) periodic. However, as localized structures develop, larger wave numbers $k_x/\kappa\sim|\Delta|^{1/2}$ are excited, and then the dynamic regime changes in a complicated man-

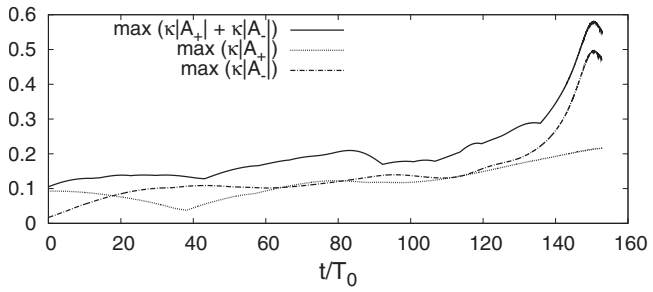

FIG. 1. The global maxima of wave amplitudes versus time.

ner. For understanding numerical results presented below, it is essential that if $|A_+|^2$ and $|A_-|^2$ differ from each other more than twice, then at relatively short scales $1 \ll \kappa l_x \lesssim |\Delta|^{-1/2}$ the nonlinear interaction in x direction is self-attractive for the dominant component, while it is repelling for the weaker component. In this regime, the dynamics is roughly described by the usual nonlinear Schroedinger equation for the dominant wave.

Also different nonlinear processes can occur in the system (7), which create instabilities near corresponding resonant curves in $\mathbf{k}$ plane. For example, two type-1 waves with $\mathbf{k}_1 = 0$ decay into two type-2 waves with wave vectors $\pm\mathbf{k}_2$ ($2 \leftrightarrow 2$ process) if $2\Omega_1(\mathbf{0}) \approx \Omega_2(\mathbf{k}_2) + \Omega_2(-\mathbf{k}_2)$. A standard linear analysis shows that a maximum of the instability increment is reached at the perpendicular direction, near $\mathbf{k}_2 = \pm \mathbf{e}_y \kappa \sqrt{8\Delta}$. However, a more detailed analytical study of Eq. (7), including full stability analysis and particular solutions, will be a subject of future research. In this work we only present results of numerical simulations (one typical example from more than ten numerical experiments carried out), which give a general impression about the dynamics, with particular attention to the phenomenon of wave collapses.

The numerical simulations were performed by a highly accurate pseudospectral method, in the standard dimensionless square domain $2\pi \times 2\pi$, with periodic boundary conditions and with $\kappa = 100$. In this example, function ε was taken in the form $\varepsilon = 0.014(1 + 0.1\cos x + 0.1\cos y)$, while $\Delta(x,y) = 0.007[1 + 0.05\xi(x,y)]$ was used, where a complex function $\xi(x,y)$ contained discrete Fourier harmonics within $-5 \le k_x \le 5$ and $-5 \le k_y \le 5$, with amplitudes decaying as $\exp[-0.1(k_x^2 + k_y^2)]$ and with pseudorandom phases (in this particular realization $0.004 \lesssim |\Delta(x,y)| \lesssim 0.01$, not shown). The initial conditions for the amplitudes were $\kappa A_+ = 0.08 + a_+(x,y)$ and $\kappa A_- = a_-(x,y)$, where functions $a_\pm(x,y)$ had the Fourier spectra with amplitudes behaving as $0.001 \exp[-0.04(k_x^2 + k_y^2)]$ and with pseudorandom phases. Thus, the most part of wave energy was initially concentrated in the forward wave. However, after few tens of wave periods, the energy has been redistributed between the forward and backward waves due to the inhomogeneous Bragg coupling (see Fig. 1). Wide regions of slightly higher wave amplitude were formed, as a result of interplay between random initial conditions and random Δ. After that, self-focusing nonlinear interactions came into play and rapidly produced the big wave which is seen in Figs. 2(b) and 3. It is interesting to note that the localized structure has developed only in one of the two

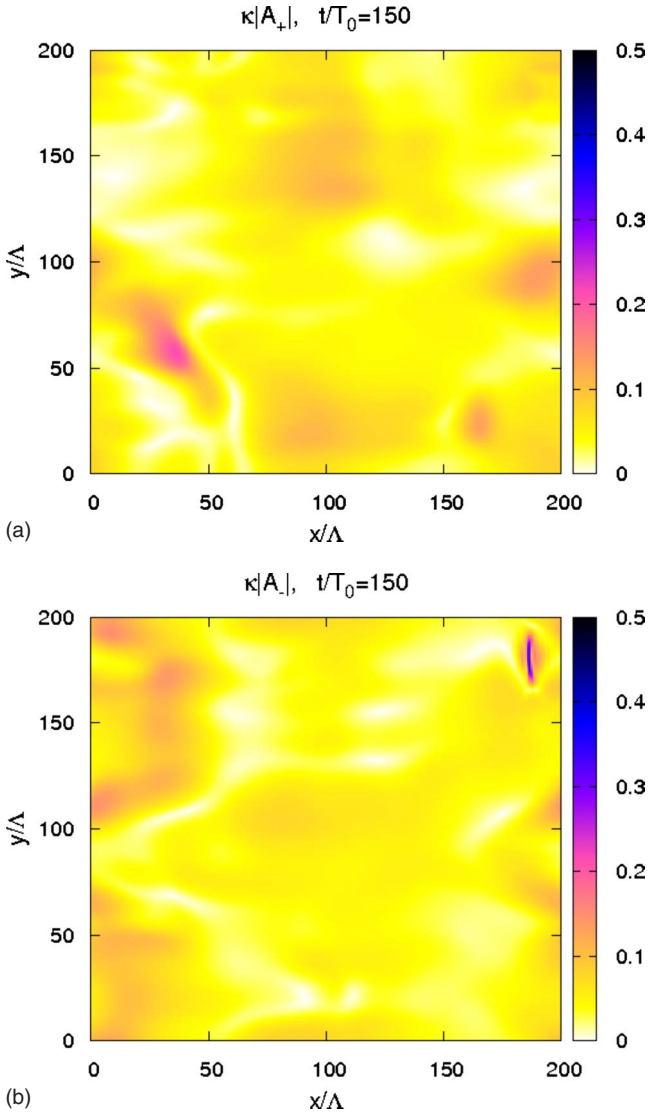

FIG. 2. (Color online) The absolute values $|A_\pm(x,y,t)|$ at $t/T_0 = 150$. The localized energetic structure is seen near the right upper corner of the $|A_-|$ map.

wave envelopes: there is no clear sign of the same big wave in the opposite-wave amplitude. This is due to the previously mentioned effect of nonlinear repelling of weak wave by much stronger opposite localized wave. The structure is moving from the right to the left, approximately with the group velocity $\tilde{\omega}/(2\kappa)$.

In some simulations, several big waves developed at different locations (in A_+ as well as in A_-), including the case of constant ε and Δ. Thus, the role of inhomogeneity is only essential in an initial stage of the evolution.

The x size of the developed high wave group contains just 1–2 wavelengths, while the y size is larger, about 10 wavelengths (see Fig. 3). The reason for such difference is that the dynamics along y in the final stage is no more focusing, as far as $|A_-|^2 - 2|A_+|^2 > 0$ in the region of collapse. Strictly speaking, the assumption of narrow spectra for $A_\pm$ is violated in this situation, so the system (7) can describe the final stage of wave collapse only qualitatively. To get indirect confirmations for the wave collapses, we compared the above

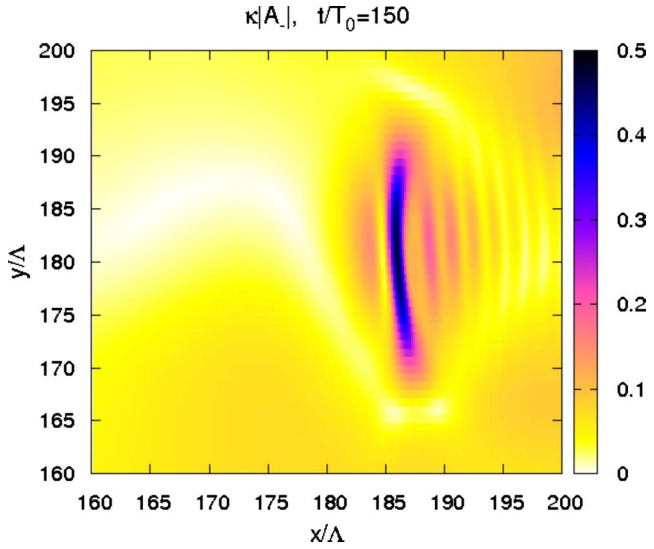

FIG. 3. (Color online) The localized structure from Fig. 2(b).

approximate results to analogous simulations of full systems of the type (4), for some simple functions $T_m(\mathbf{k}_1,\mathbf{k}_2;\mathbf{k}_3,\mathbf{k}_4)$ which possess the same property (5) and thus mimic the true complicated matrix element $T(\mathbf{k}_1,\mathbf{k}_2;\mathbf{k}_3,\mathbf{k}_4)$. In particular, we considered $T_m \propto |\mathbf{k}_1|^{\frac{1}{2}}|\mathbf{k}_2|^{\frac{1}{2}}|\mathbf{k}_3|^{\frac{1}{2}}|\mathbf{k}_4|^{\frac{1}{2}}(|\mathbf{k}_1+\mathbf{k}_2|+|\mathbf{k}_3+\mathbf{k}_4| -|\mathbf{k}_1-\mathbf{k}_3|-|\mathbf{k}_1-\mathbf{k}_4|-|\mathbf{k}_2-\mathbf{k}_3|-|\mathbf{k}_2-\mathbf{k}_4|)$, and there the wave collapses were observed as well (we do not discuss here subtle points related to such systems). In the reality, however, higher-order nonlinearities become important at $|\kappa A_\pm| \gtrapprox 0.3$ and they produce wave breaking manifested as the well-known "white caps." Therefore the question about maximal wave height at the finite stage of collapse can be fully answered only through real-world experiments.

To conclude, in the present work we have derived and then numerically simulated nonlinear equations of motion for complex water wave amplitudes coupled both linearly through the (spatially nonuniform) Bragg interaction, and nonlinearly through the cross-modulation terms. In the numerical experiments, we have observed spontaneous formation of highly energetic localized structures which look like wave collapses rather than like solitons (no quasistationary regime was observed). The final stage of these collapses is actually beyond applicability of our model. That is why some real-world experiments or at least fully nonlinear simulations are desirable. Unfortunately, large-scale simulations in the framework of the exact Eulerian dynamics, for instance with the help of the existing boundary integral methods, are hardly possible at the moment because of their extremely time-demanding implementations. Perhaps, the weakly nonplanar but fully nonlinear equations of motion for potential water waves over quasi-one-dimensional topography, derived in Ref. [27], or alternatively the method by Guyenne and Nicholls [28], might be useful as an intermediate step toward accurate numerical results.

These investigations were supported by RFBR (Grants No. 09-01-00631 and No. 07-01-92165), by the "Leading Scientific Schools of Russia" Grant No. 4887.2008.2, and by the Program "Fundamental Problems of Nonlinear Dynamics" from the RAS Presidium.

[1] W. Chen and D. L. Mills, Phys. Rev. Lett. **58**, 160 (1987).
[2] A. B. Aceves and S. Wabnitz, Phys. Lett. A **141**, 37 (1989).
[3] B. J. Eggleton, R. E. Slusher, C. M. de Sterke, P. A. Krug, and J. E. Sipe, Phys. Rev. Lett. **76**, 1627 (1996).
[4] D. N. Christodoulides and R. I. Joseph, Phys. Rev. Lett. **62**, 1746 (1989).
[5] T. Peschel, U. Peschel, F. Lederer, and B. A. Malomed, Phys. Rev. E **55**, 4730 (1997).
[6] I. V. Barashenkov, D. E. Pelinovsky, and E. V. Zemlyanaya, Phys. Rev. Lett. **80**, 5117 (1998).
[7] A. De Rossi, C. Conti, and S. Trillo, Phys. Rev. Lett. **81**, 85 (1998).
[8] C. Conti, S. Trillo, and G. Assanto, Phys. Rev. Lett. **85**, 2502 (2000).
[9] T. Iizuka and C. Martijn de Sterke, Phys. Rev. E **61**, 4491 (2000).
[10] C. Conti and S. Trillo, Phys. Rev. E **64**, 036617 (2001).
[11] K. W. Chow, I. M. Merhasin, B. A. Malomed *et al.*, Phys. Rev. E **77**, 026602 (2008).
[12] N. K. Efremidis and D. N. Christodoulides, Phys. Rev. A **67**, 063608 (2003).
[13] D. E. Pelinovsky, A. A. Sukhorukov, and Yu. S. Kivshar, Phys. Rev. E **70**, 036618 (2004).
[14] M. Matuszewski, W. Krolikowski, M. Trippenbach, and Y. S. Kivshar, Phys. Rev. A **73**, 063621 (2006).
[15] V. P. Ruban, Phys. Rev. E **77**, 055307(R) (2008).
[16] V. P. Ruban, Phys. Rev. E **78**, 066308 (2008).
[17] V. P. Ruban, Phys. Rev. E **70**, 066302 (2004).
[18] C. Kharif and E. Pelinovsky, Eur. J. Mech. B/Fluids **22**, 603 (2003).
[19] E. Pelinovsky and C. Kharif, Eur. J. Mech. B/Fluids **25** (5), 535 (2006), special issue of Rogue Waves, edited by E. Pelinovsky and C. Kharif.
[20] C. C. Mei and Y. Li, Phys. Rev. E **70**, 016302 (2004).
[21] J. Garnier, R. A. Kraenkel, and A. Nachbin, Phys. Rev. E **76**, 046311 (2007).
[22] R. A. Smith, J. Fluid Mech. **363**, 333 (1998).
[23] V. P. Krasitskii, J. Fluid Mech. **272**, 1 (1994).
[24] V. Zakharov, Eur. J. Mech. B/Fluids **18**, 327 (1999).
[25] M. Onorato, A. R. Osborne, and M. Serio, Phys. Rev. Lett. **96**, 014503 (2006).
[26] P. K. Shukla, I. Kourakis, B. Eliasson, M. Marklund, and L. Stenflo, Phys. Rev. Lett. **97**, 094501 (2006).
[27] V. P. Ruban, Phys. Rev. E **71**, 055303(R) (2005).
[28] P. Guyenne and D. P. Nicholls, SIAM J. Sci. Comput. **30**, 81 (2007).